Pergamon

Int. J. Solids Structures Vol. 33, No. 20–22, pp. 2969–2992, 1996

0020–7683/96 $15.00 + .00

0020–7683(95)00252–9

A UNIFIED CO-ROTATIONAL FRAMEWORK FOR SOLIDS, SHELLS AND BEAMS

M. A. CRISFIELD
Dept of Aeronautics, Imperial College, London, U.K.

and

G. F. MOITA
FEA Ltd, Kingston upon Thames, Surrey, U.K.

Abstract—The paper describes a unified framework for applying the co-rotational method to the analysis of solids, shells and beams. The general method stems from an unusual application of the technique which involves solid elements.

The proposed framework allows a formulation that is simpler than many of the earlier procedures and, in addition, gives a direct indication of the terms in the tangent stiffness which may be ignored. Copyright © 1996 Elsevier Science Ltd.

INTRODUCTION

The co-rotational method was originally introduced by Wempner (1969) and Belytschko and co-workers (1973, 1979) and has much in common with the "natural approach" of Argyris *et al.* (1979). Important early work on beams was also due to Oran (1973a, 1973b) although the co-rotational basis was somewhat obscured by the introduction of "beam-column" terms.

Although most work with the co-rotational technique has involved beams and shells (i.e. Belytschko (1973, 1979), Crisfield *et al.* (1990, 1992), Nour-Omid *et al.* (1991), Nygard *et al.* (1989), Oran (1973a, 1973b), Hsiao (1987), Peng *et al.* (1992), Rankin *et al.* (1986)) in 1991, Jetteur and Cescotto applied a form of co-rotational procedure to two-dimensional continuum elements. Following the latter work, the authors have applied the co-rotational technique to both two and three-dimensional solid elements [Crisfield *et al.* (1995 and submitted), Moita *et al.* (1994 and submitted)]. The key motivation was very similar to that driving much of the work on beams and shells—a desire to be able to directly utilise the very considerable research effort that has been put into the development of effective linear elements. Using the co-rotational technique, this can be simply achieved if the local element response involves small strains. Even with large strains, there are signs that the co-rotational technique can be a useful platform [Moita (1994), Crisfield *et al.* (1995)] although the variations of rotation over an element must then be small. The current work will be limited to small strains although the possible later extension to large-strains will be borne in mind.

The first author's earlier work using the co-rotational formulation (Crisfield *et al.* (1990, 1991, 1992)) adopted the technique whereby, at the element level, the local formulation only directly involved the local strain producing displacements (having removed those involving the rigid-body modes). The co-rotational aspects then became closely enmeshed with the local element behaviour. In the current work, we have returned to a procedure pioneered by Rankin and Brogan (1986) in which the co-rotational computations are totally divorced from the local element computations. This "element independent

approach" has important coding advantages. However, if the local element exactly satisfies the usual linear strain-free rigid body requirements, there will be no difference between the results or convergence characteristics using the two approaches.

Our recent work on continua has made us re-visit earlier work on beams (Crisfield (1990) and shells (Peng and Crisfield (1992)) with a view to simpler derivations. In particular, we now not only apply an "element independent formulation", but also introduce terms involving the spin of the local frame. Using this approach, which has strong links with earlier work by Nour-Omid and Rankin (1991), a common framework can be developed for a range of different types of element. In addition, the method directly introduces a convenient procedure for deciding which terms to omit in the derivation of the tangent stiffness matrices.

The paper will initially consider three-dimensional continuum elements because this work provided the motivation for the current framework. We will then turn to shells. Although the work on shells is based on the co-rotational approach, some of the concepts have a wider application. In particular, three separate approaches are adopted for dealing with the "drilling rotation". In the first, the issue is effectively ignored and the problem is formulated directly in terms of nodes with three rotational variables. Because the method is based on the co-rotational procedure, the issue of the drilling rotation is left to the embedded linear element which is assumed to have an in-plane rotational stiffness. This stiffness may be "real" if the element directly incorporates "drilling variables" (Bergan *et al.* (1986), MacNeal *et al.* (1988)). Alternatively, the stiffness may be left as zero in which case singularities may arise as the curvature of the system approaches zero and the system becomes planar or as the mesh is refined. As another alternative, the approach of Zienkiewicz *et al.* (1968) may be adopted so that an artificial stiffness is introduced. However, in a non-linear environment, there are likely to be problems with such an approach in which the artificial stiffness is related to the real stiffness of the adjacent elements. In particular, these problems may arise when plasticity is involved.

An alternative procedure for handling the issue of the "drilling rotation" is to only include three rotation variables at branched intersections (in contrast to the previous technique, a more complex "house keeping" is required). Away from intersections, assuming the shell to be smooth, only two rotational variables are included. In a non-linear context, the method can be considered to have its origins in an important early paper in Horrigmoe and Bergan (1978). However, unlike the latter work, the accuracy of the current work does not depend on the assumption of small increments. With respect to its treatment of the rotational variables, the present procedure has much in common with the procedure of Simo *et al.* (1989a, 1989b, 1990b, 1993b) and Celigoj (submitted).

Yet another procedure for dealing with the problem of the "drilling rotation" is to avoid such rotations and instead use a single rotation about an element side. This is the procedure adopted in both the "Morley triangle" (Morley (1971)) and in Irons's semi-loof elements (Irons (1976)). Non-linear formulations for the Morley triangle have been given by Peng and Crisfield (1992) and by van Keulen *et al.* (1993). The present paper will include a re-working of the former formulation which puts it within the context of the current "general framework". A similar re-working will also be applied to the co-rotational procedure for three-dimensional beams (Crisfield (1990)).

It has already been stated that one of the objectives of the corotational formulation is to allow the analyst to use whichever of the better linear element formulations he or she chooses. As an example in the work with continua elements (Crisfield *et al.* (1995 and submitted), Moita *et al.* (1994 and submitted)), we have used "incompatible modes" (Taylor *et al.* (1976)) or "enhanced strains" (Simo *et al.* (1990a)) to improve the performance. However, in the present paper we will not be concerned with these aspects because the paper will concentrate on the description of the surrounding "co-rotational harness". Details on the numerical performance of the co-rotational elements can be found elsewhere (Crisfield *et al.* (1990, 1995 and submitted), Moita *et al.* (1994 and submitted), Peng *et al.* (1992)). In relation to beams and shells, these numerical results (Crisfield (1990), Peng and Crisfield (1992)) relate to the earlier co-rotational formulation. We have yet to demonstrate numerically that the results are similar for the current formulation.

FRAMEWORK FOR THE "ELEMENT INDEPENDENT" FORMULATION

We should start by pointing out that the "element independence" (Rankin *et al.* (1986)) relates to a particular class of element with the same "connectivity". In other words, the work that will be described on three-dimensional brick elements will relate to any eight-noded brick element, no matter what enhancements or internal variables are included. In a similar manner, the work on triangular shell elements with three nodes and six variables per node will be applicable to any such linear elements.

As a start, it will be assumed that we are given the co-ordinate axes for the local co-rotating frame, which are defined by the three-unit vectors $\mathbf{e}_1$–$\mathbf{e}_3$, as well as the element nodal displacement vector in global co-ordinates, $\mathbf{p}$. Given this information, we can (at the element level) find the local nodal displacement vector, $\mathbf{p}_l$, via:

$$\mathbf{p}_l = f(\mathbf{p}, \mathbf{e}_1, \mathbf{e}_2, \mathbf{e}_3) \tag{1}$$

Throughout the paper the subscript l will be used for "local" while if no subscript is given, the quantity is assumed to be "global". We will assume that (1) can be differentiated so that we can obtain the transformation matrix $\mathbf{T}$ whereby:

$$\delta\mathbf{p}_l = \mathbf{T}\delta\mathbf{p} \tag{2}$$

while the equivalence of the virtual work in the local and global systems leads to the relationship:

$$\mathbf{q}_i = \mathbf{T}^{\mathrm{T}}\mathbf{q}_{il} \tag{3}$$

where the local internal force vector, $\mathbf{q}_{il}$ is given by the conventional relationship:

$$\mathbf{q}_{il} = \int \mathbf{B}_l^{\mathrm{T}}\sigma_l \,\mathrm{d}V_o = \mathbf{K}_l\mathbf{p}_l \tag{4}$$

where $\mathbf{B}_l$ is the conventional linear strain/nodal displacement matrix and σ_l are the equivalent stresses. The last expression in (4) only applies if a linear relationship is assumed at the local level. (The method is easily modified to allow for non-linear relationships, including plasticity at the local element level (Crisfield *et al.* (1992 and to be published).) Assuming such a linear relationship, from (3) and (4) we then obtain:

$$\mathbf{q}_i = \mathbf{T}^{\mathrm{T}}\mathbf{K}_l\mathbf{p}_l \tag{5}$$

To obtain the global tangent stiffness matrix, differentiation of (3) leads to the relationship:

$$\delta\mathbf{q}_i = \mathbf{T}^{\mathrm{T}}\delta\mathbf{q}_{il} + \delta\mathbf{T}^{\mathrm{T}}\mathbf{q}_{il} = \mathbf{T}^{\mathrm{T}}\mathbf{K}_{tl}\delta\mathbf{p}_l + \mathbf{K}_{t\sigma}\delta\mathbf{p}_g = \mathbf{T}^{\mathrm{T}}\mathbf{K}_{tl}\mathbf{T}\delta\mathbf{p}_l + \mathbf{K}_{t\sigma}\delta\mathbf{p}_g \tag{6}$$

where we have included a subscript t or tangential on $\mathbf{K}_{tl}$ to allow for the possibility of "local non-linearity". In the following developments, we will specify the transformation matrix $\mathbf{T}$ and the initial stress matrix, $\mathbf{K}_{t\sigma}$, for a range of applications.

3-D CONTINUA

The initial co-rotating local co-ordinates are set equal to the initial co-ordinates minus those at node 1 so that at node j:

$$\mathbf{X}_l^j = \mathbf{X}^j - \mathbf{X}^1 \tag{7}$$

(Note. In this and in many subsequent equations, the node numbers have been placed as

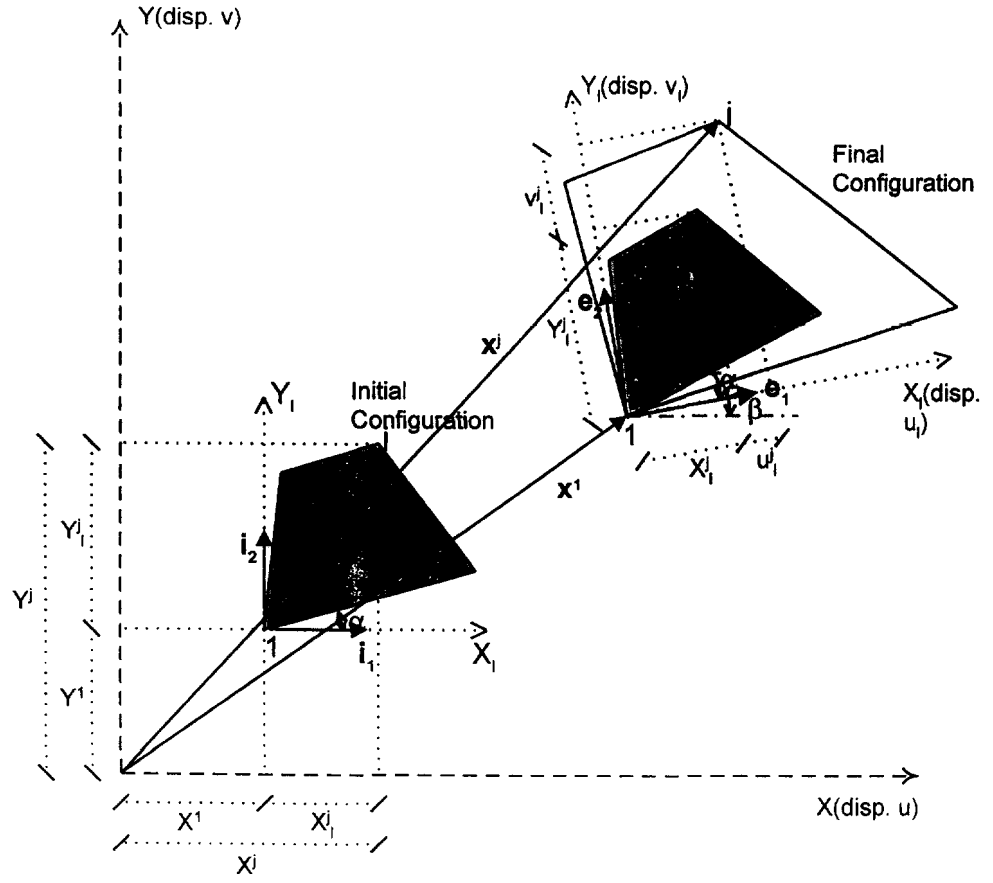

Fig. 1. Initial and final configurations—rotation and stretch.

postscripts. This is purely for convenience to avoid a clash with the subscript l for local. However, where such a potential clash would not arise, we will sometimes revert to using subscripts for node numbers.) In order to explain the adopted process, we will firstly consider the two-dimensional situation illustrated in Fig. 1. If we assume, for the present, that the local rotating unit vectors, $\mathbf{e}_1$ and $\mathbf{e}_2$ are known, then from Fig. 1, by writing the current position vector of node j in two separate ways, we can obtain:

$$\mathbf{x}_l^j = \mathbf{X}_l^j + \mathbf{d}_l^j = \begin{pmatrix} \mathbf{X}_l \\ \mathbf{Y}_l \end{pmatrix}^j + \begin{pmatrix} u_l \\ v_l \end{pmatrix}^j = \mathbf{E}^{\mathrm{T}}(\mathbf{x}^j - \mathbf{x}^1) = \mathbf{E}^{\mathrm{T}}\mathbf{x}^{j1} = \mathbf{E}^{\mathrm{T}}\begin{pmatrix} x \\ y \end{pmatrix}^{j1} \tag{8}$$

where it would be possible to make the vector $\mathbf{e}_1$ coincide with one of the sides of the element. However the formation would not then be invariant with respect to the scheme that is adopted for ordering the node numbers. This need not be a serious problem for small strain analysis. However, we would later like to extend the method to large strain analyses (Crisfield *et al.* (1995)). With this in mind, we will choose the local axes so that the element can pass the "large-strain patch test" which was originally proposed by Jetteur and Cescotto (1991) and later defined by Simo *et al.* (1993b) as requiring "the exact solution for homogeneous deformations with constant deformation gradient F".

In two dimensions, a procedure for successfully choosing the local axes was originally proposed by Jetteur and Cescotto (1991) and is illustrated in Fig. 2 for a shearing deformation. The method ensures that the local "spin" at the centre of the element is zero, i.e.

$$\Omega_{lm} = \left(\frac{\partial u}{\partial Y} - \frac{\partial v}{\partial X}\right)_{lm} = 0 \tag{9}$$

In order to extend the previous formulation to three-dimensions, it will be shown that the

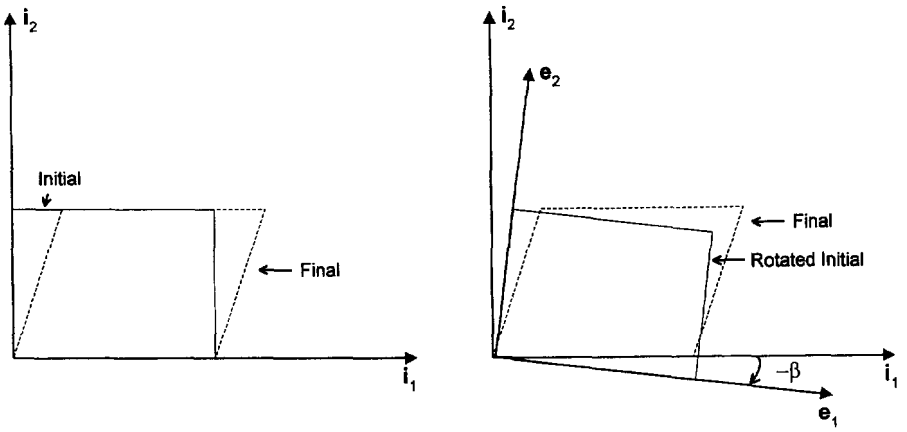

Fig. 2. Example with local axes $\mathbf{e}_1$ and $\mathbf{e}_2$.

previous procedure for computing the local rotating base vectors $\mathbf{e}_1$ and $\mathbf{e}_2$ (now also $\mathbf{e}_3$), is equivalent to the computation of:

$$\mathbf{E} = [\mathbf{e}_1\mathbf{e}_2\mathbf{e}_3] = \mathbf{R}_m \tag{10}$$

where

$$\mathbf{F}_m = \mathbf{R}_m\mathbf{U}_m \tag{11}$$

involves a polar decomposition at the centroid (or "middle"—hence the subscript m) of the element. To demonstrate this assertion, we begin with the deformations shown in Fig. 3. If we compare Fig. 1 with Fig. 3, we note that they are equivalent with the latter illustrating a process whereby the element is strained and later rotated while the former represents a rotation followed by a stretch.

From Figs 1 and 3, at the centroid of the element, we can write:

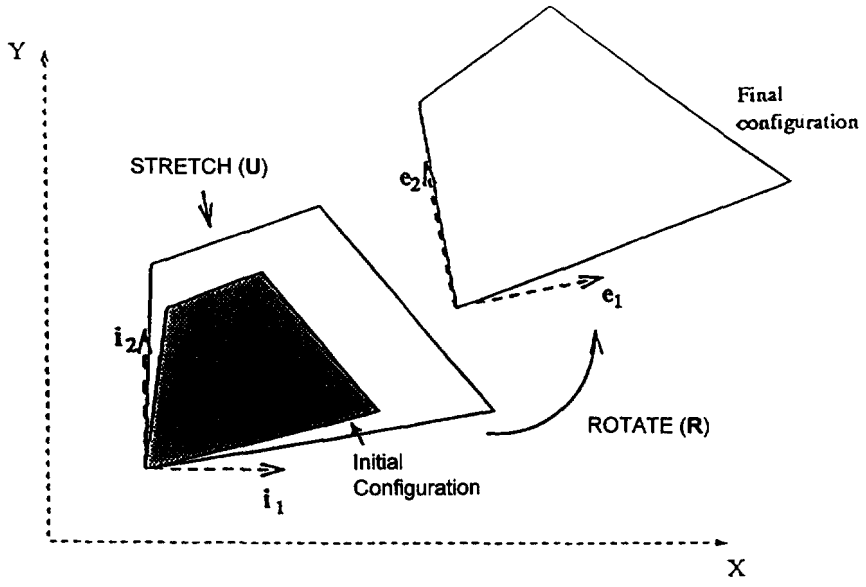

Fig. 3. Polar decomposition—stretching preceding the rotation.

$$\mathbf{U}_m = \left[\frac{\partial \mathbf{x}_l}{\partial \mathbf{X}_l}\right]_m = \left[\mathbf{I} + \frac{\partial \mathbf{u}_l}{\partial \mathbf{X}_l}\right]_m = \mathbf{I} + \mathbf{D}_{lm} \tag{12}$$

Here $\mathbf{x}_l = \mathbf{X}_l + \mathbf{u}_l$ and $\mathbf{D}_{lm}$ is the local displacement derivative matrix.

We can also write the local engineering strain (still at the centroid) as:

$$\boldsymbol{\varepsilon}_{lm} = \tfrac{1}{2}(\mathbf{D}_{lm} + \mathbf{D}_{lm}^{\mathrm{T}}) \tag{13}$$

Equations (12) and (13) lead to an expression for the local engineering strain of the form:

$$\boldsymbol{\varepsilon}_{lm} = \tfrac{1}{2}\mathbf{U}_m + \tfrac{1}{2}\mathbf{U}_m^{\mathrm{T}} - \mathbf{I} = \mathbf{U}_m - \mathbf{I} \tag{14}$$

which shows that $\boldsymbol{\varepsilon}_{lm}$ can be considered as a Biot strain. In (14) we have used the property of the symmetry of the right stretch matrix $\mathbf{U}$ so that $\mathbf{D}_{lm} = \mathbf{D}_{lm}^{\mathrm{T}}$. In the two dimensional case, the latter relationship is entirely equivalent to (9).

In practice, we do not compute the local strains from (14) but rather (at the Gauss points) from the local displacements $\mathbf{p}_l$ obtained from the $\mathbf{d}_l^j$ of (8) with the aid of the $\mathbf{E}$ matrix previously computed from (10) and (11) using a polar decomposition at the centroid of the element. For the current eight noded brick element, the element local displacement vector is given by:

$$\mathbf{p}_l^{\mathrm{T}} = (\mathbf{d}_l^{1\mathrm{T}}, \mathbf{d}_l^{2\mathrm{T}}, \ldots \mathbf{d}_l^{8\mathrm{T}}) \tag{15}$$

with a similar expression for the global quantities.

To obtain the important transformation matrix $\mathbf{T}$, we differentiate (8) to obtain:

$$\delta \mathbf{d}_l^j = \mathbf{E}^{\mathrm{T}} \delta \mathbf{d}^{j1} + \delta \mathbf{E}^{\mathrm{T}} \mathbf{x}^{j1} \tag{16}$$

Equation (16) ensures that $\delta \mathbf{d}_l^1$ is zero. However, the subsequent equations turn out to be simpler if we work with a modified set of local displacement changes, which are obtained by adding $\mathbf{E}^{\mathrm{T}} \delta \mathbf{d}_1$ to each nodal displacement change vector. If the local element computations correctly satisfy the strain-free rigid-body requirements, this modification should have no effect. We will now apply this modification and also introduce the relationship:

$$\delta \mathbf{E} = \mathbf{S}(\delta \boldsymbol{\beta}) \mathbf{E} \tag{17}$$

where $\mathbf{S}(\delta \boldsymbol{\beta})$ is the skew symmetric matrix of the spin vector, $\delta \boldsymbol{\beta}$, which will be found shortly. The matrix $\mathbf{S}(\delta \boldsymbol{\beta})$ is given by:

$$\mathbf{S}(\delta \boldsymbol{\beta}) = \begin{bmatrix} 0 & -\delta\beta_3 & \delta\beta_2 \\ \delta\beta_3 & 0 & -\delta\beta_1 \\ -\delta\beta_2 & \delta\beta_1 & 0 \end{bmatrix} \tag{18}$$

Substituting from (17) into the modified version of (16) (with $\delta \mathbf{d}^j$ instead of $\delta \mathbf{d}^{j1}$), we obtain:

$$\delta \mathbf{d}_l^j = \mathbf{E}^{\mathrm{T}} \delta \mathbf{d}^j + \mathbf{E}^{\mathrm{T}} \mathbf{S}(\mathbf{x}^{j1}) \delta \boldsymbol{\beta} \tag{19}$$

To obtain an expression for $\delta \boldsymbol{\beta}$, we note that, using the element shape functions, we can obtain:

$$\mathbf{v}(\Omega_{lm}) = \sum \mathbf{A}_l^j \mathbf{d}_l^j = 0 \tag{20}$$

where the 3×1 vector $\mathbf{v}(\Omega_{lm})$ is the vector equivalent of $\mathbf{D}_{lm} - \mathbf{D}_{lm}^{\mathrm{T}}$ (see (12)) and is obtained

at the centroid of the element. The terms $\mathbf{A}_l$ in (20) are functions of the initial local co-ordinates $\mathbf{X}_l$ which are fixed. Differentiation of (20) and substitution from (19) leads to:

$$\delta \mathbf{v}(\Omega_{lm}) = \sum \mathbf{A}_l^j \delta \mathbf{d}_l^j = \sum \mathbf{A}_l^j \mathbf{E}^{\mathrm{T}} \delta \mathbf{d}^j + \sum \mathbf{A}_l^j \mathbf{E}^{\mathrm{T}} \mathbf{S}(\mathbf{x}^{j1}) \delta \boldsymbol{\beta} = 0 \tag{21}$$

from which:

$$\delta \boldsymbol{\beta} = -\left[\sum \mathbf{A}_l^j \mathbf{E}^{\mathrm{T}} \mathbf{S}(\mathbf{x}^{j1})\right]^{-1} \sum \mathbf{A}_l^j \mathbf{E}^{\mathrm{T}} \delta \mathbf{d}_j = \mathbf{V}^{\mathrm{T}} \delta \mathbf{p} \tag{22}$$

where the "spin matrix" $\mathbf{V}^{\mathrm{T}}$ is of dimension 3×24 (assuming an eight noded brick element).

Equation (22) can now be substituted into (19) so that:

$$\delta \mathbf{p}_l = \mathbf{T} \delta \mathbf{p} = [[\mathrm{Diag}\, \mathbf{E}^{\mathrm{T}}] \delta \mathbf{p} + \mathrm{Diag}\, \mathbf{E}^{\mathrm{T}}\, \mathrm{col}(\mathbf{S}(\mathbf{x}^{j1})) \mathbf{V}^{\mathrm{T}}] \delta \mathbf{p} \tag{23}$$

where $\mathrm{Diag}\, \mathbf{E}^{\mathrm{T}}$ is of magnitude 24×24 with eight 3×3 sub-matrices $\mathbf{E}^{\mathrm{T}}$ on the diagonal while $\mathrm{col}\{\mathbf{S}(\mathbf{x}^{j1})\}$ is a 24×3 matrix consisting of eight sub-matrices $\mathbf{S}(\mathbf{x}^{j1})$ as j moves from one to the number of nodes, which is here eight. Using (23), the global internal force vector, $\mathbf{q}_i = \mathbf{T}^{\mathrm{T}} \mathbf{q}_l$, can be expressed as:

$$\mathbf{q}_i = \mathrm{col}(\mathbf{E}\mathbf{q}_{li}^j) - \mathbf{V}\, \mathrm{row}(\mathbf{S}(\mathbf{x}^{j1}))\, \mathrm{col}(\mathbf{E}\mathbf{q}_{li}^j) = \mathrm{col}(\bar{\mathbf{q}}_{li}^j) - \mathbf{V}\, \mathrm{row}(\mathbf{S}(\mathbf{x}^{j1}))\, \mathrm{col}(\bar{\mathbf{q}}_{li}^j) \tag{24}$$

The terms following $\mathbf{V}$ in (24) represent three rotational equilibrium equations for the element of the form:

$$\mathbf{a} = \sum \mathbf{x}^{j1} \times \bar{\mathbf{q}}_{li}^j = 0 \tag{25}$$

where $\bar{\mathbf{q}}_{li}^j$ are the local element nodal forces with respect to the global axes. Clearly, at equilibrium the vector $\mathbf{a}$ will be zero so that the term following $\mathbf{V}$ in (24) will vanish at equilibrium. Both here and in the subsequent work on shells and beams, we will use this observation as a justification for ignoring the $\delta \mathbf{V}$ terms in the following derivation of the initial stress matrix. (It is, however, worth noting that while in the two-dimensional case, the full formulation (including terms from $\delta \mathbf{V}$) leads to a symmetric stiffness matrix (Crisfield *et al.* (submitted), Moita (1994)), this is not true of the three-dimensional formulation for which a non-symmetric tangent stiffness matrix results (Moita *et al.* (1994 and submitted)).

The tangent stiffness matrix is composed of a conventional term $\mathbf{T}^{\mathrm{T}} \mathbf{K}_l \mathbf{T}$ (see (6)) and an initial stress contribution, with the latter stemming from the differentiation of (24) with $\mathbf{q}_{li}$ fixed. The latter process leads to:

$$\delta \mathbf{q}_i = \mathrm{col}(\delta \mathbf{E}\mathbf{q}_{li}^j) - \mathbf{V}\, \mathrm{row}(\mathbf{S}(\delta \mathbf{x}^{j1}))\, \mathrm{col}(\mathbf{E}\mathbf{q}_{li}^j) - \mathbf{V}\, \mathrm{row}(\mathbf{S}(\mathbf{x}^{j1}))\, \mathrm{col}(\delta \mathbf{E}\mathbf{q}_{li}^j) \tag{26}$$

With the aid of (17) and (22) we now obtain:

$$\mathbf{K}_{t\sigma} = -\mathrm{col}(\mathbf{S}(\bar{\mathbf{q}}_{li}^j)) \mathbf{V}^{\mathrm{T}} + \mathbf{V}\, \mathrm{row}(\mathbf{S}(\bar{\mathbf{q}}_{li}^j)) + \mathbf{V}\, \mathrm{row}(\mathbf{S}(\mathbf{x}^{j1}))\, \mathrm{col}(\mathbf{S}(\bar{\mathbf{q}}_{li}^j)) \mathbf{V}^{\mathrm{T}} \tag{27}$$

The first term is the transpose of the second term but the third term is in general non-symmetric because the central 3×3 component can be written as:

$$\sum \mathbf{S}(\mathbf{x}^{j1}) \mathbf{S}(\bar{\mathbf{q}}_{li}^j) = \sum (\mathbf{x}^{j1} \bar{\mathbf{q}}_{li}^{j\mathrm{T}} - (\mathbf{x}^{j1\mathrm{T}} \bar{\mathbf{q}}_{li}^j) \mathbf{I}) \tag{28}$$

The non-symmetric part of (28) is:

$$\text{Non-sym} = \frac{1}{2}\sum (\mathbf{x}^{j1}\bar{\mathbf{q}}_{li}^{j\mathrm{T}} - \bar{\mathbf{q}}_{li}^{j}\mathbf{x}^{j1\mathrm{T}}) \tag{29}$$

However, as previously discussed, at equilibrium the term after $\mathbf{V}$ in the last term of (24) will be zero (see (25)) and in addition:

$$\mathbf{S}(\mathbf{a}) = \sum \mathbf{S}(\mathbf{x}^{j1} \times \bar{\mathbf{q}}_{li}^{j}) = \sum (\mathbf{x}^{j1}\bar{\mathbf{q}}_{li}^{j\mathrm{T}} - \bar{\mathbf{q}}_{li}^{j}\mathbf{x}^{j1\mathrm{T}}) = 0 \tag{30}$$

It follows that the non-symmetric term (29) will vanish at equilibrium and we will be justified in using the symmetric part of the tangent stiffness matrix in (27) for our Newton-Raphson iterations so that:

$$\mathbf{K}_{t\sigma} = -\text{col}(\mathbf{S}(\bar{\mathbf{q}}_{li}^{j}))\mathbf{V}^{\mathrm{T}} + \mathbf{V}\,\text{row}(\mathbf{S}(\bar{\mathbf{q}}_{li}^{j})) + \mathbf{V}\,\text{sym}\left(\sum (\mathbf{S}(\mathbf{x}^{j1})\mathbf{S}(\bar{\mathbf{q}}_{li}^{j}))\right)\mathbf{V}^{\mathrm{T}} \tag{31}$$

Numerical experiments support this contention and show that an excellent (quadratic) rate of convergence is achieved (Moita (1994)). A theoretical justification has been given by Nour-Omid and Rankin (1991) who prove that a formulation which becomes symmetric at equilibrium will still exhibit "quadratic convergence" if artificially symmetrised away from equilibrium.

A TRIANGULAR SHELL FORMULATION WITH THREE ROTATIONAL VARIABLES PER NODE

We will firstly consider a curved triangular shell composed of simple triangles by means of facet approximation (Fig. 4). We will again choose the origin of the co-rotating system at node 1. The $\mathbf{e}_3$ vector is simply chosen as being orthogonal to the current facet (Fig. 4). The most easy way to choose the two remaining vectors $\mathbf{e}_1$ and $\mathbf{e}_2$ would be to make one of them coincide with one of the current sides of the element so that:

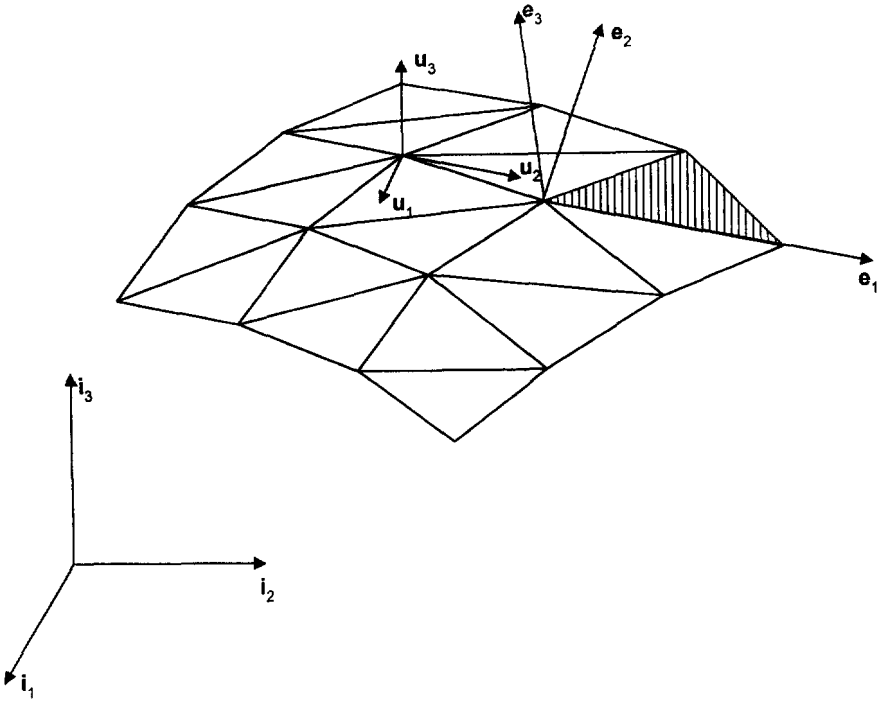

Fig. 4. Triangular facet approximation to curved shell with first choice local element frame $[\mathbf{e}_1, \mathbf{e}_2, \mathbf{e}_3]$ and nodal surface triad $\mathbf{U}_s = [\mathbf{u}_1, \mathbf{u}_2, \mathbf{u}_3]$.

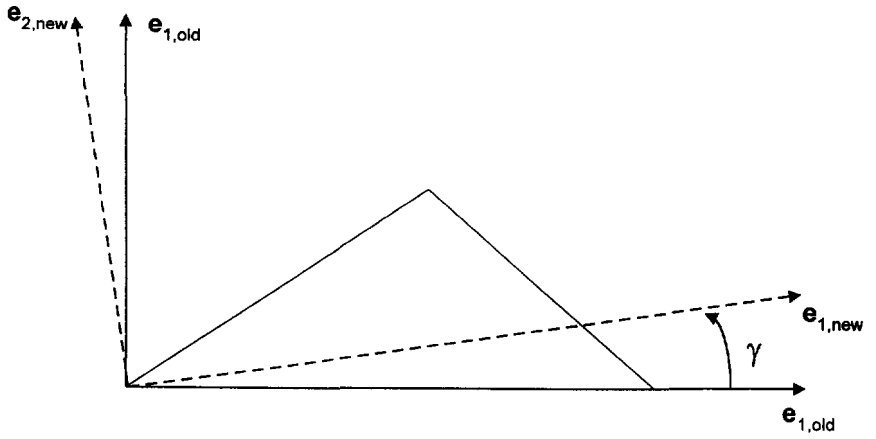

Fig. 5. Modifying first-choice (old) frame to new element frame.

$$\mathbf{e}_1 = \frac{\mathbf{x}_2 - \mathbf{x}_1}{\| \mathbf{x}_2 - \mathbf{x}_1 \|} = \frac{\mathbf{x}_{21}}{\| \mathbf{x}_{21} \|}; \quad \mathbf{e}_3 = \frac{\mathbf{x}_{21} \times \mathbf{x}_{31}}{\| \mathbf{x}_{21} \| \, \| \mathbf{x}_{31} \|}; \quad \mathbf{e}_2 = \mathbf{e}_3 \times \mathbf{e}_1 \tag{32}$$

In the initial configuration, the local initial nodal co-ordinates, $\mathbf{X}_l^j$, would then be computed with respect to this initial element frame and would be kept fixed as the co-rotating local initial co-ordinates.

In the current configuration, with a view to possible later extensions to large strains and in order to make invariant to the adopted node numbering, we will follow the previous approach of making the local spin zero. To this end, we could start with an initial set of current base vectors obtained from (32) in the current configuration and then use (8) to obtain initial values for the nodal displacements $\mathbf{d}_l^j$ at each of the nodes j and hence obtain initial estimates for the local nodal displacement vector $\mathbf{p}_l$. At which point the local displacements derivatives (4×1) can be obtained and hence the matrix equivalent $\mathbf{D}_l(2 \times 2)$. To obtain the new $\mathbf{e}_1$ and $\mathbf{e}_2$ with respect to the old ones (Fig. 5), we can (via (11) and (12)) write:

$$\mathbf{U} = \mathbf{R}^{\mathrm{T}}\mathbf{F} = \begin{bmatrix} \cos\gamma & \sin\gamma \\ -\sin\gamma & \cos\gamma \end{bmatrix} [\mathbf{I} + \mathbf{D}_l] \tag{33}$$

so that the condition $\mathbf{U}(1,2) = \mathbf{U}(2,1)$ leads to:

$$-\sin\gamma\left(1 + \left(\frac{\partial u}{\partial \mathbf{X}}\right)_l\right) + \cos\gamma\left(\frac{\partial v}{\partial \mathbf{X}}\right)_l = \cos\gamma\left(\frac{\partial u}{\partial \mathbf{Y}}\right)_l + \sin\gamma\left(1 + \left(\frac{\partial v}{\partial \mathbf{Y}}\right)_l\right) \tag{34}$$

from which we can obtain the angle γ and hence the new axes (Fig. 5):

$$\begin{aligned} \mathbf{e}_{1\mathrm{new}} &= \cos\gamma \mathbf{e}_{1\mathrm{old}} + \sin\gamma \mathbf{e}_{2\mathrm{old}} \\ \mathbf{e}_{2\mathrm{new}} &= -\sin\gamma \mathbf{e}_{1\mathrm{old}} + \cos\gamma \mathbf{e}_{2\mathrm{old}} \end{aligned} \tag{35}$$

while the $\mathbf{e}_3$ vector is unaltered.

The local displacements can now be re-computed (via (8)) using the new base vectors. In the future developments, we will not use the subscript "new" but it will be implied whenever the base vectors are referred to. In order to proceed further, it is necessary to find an expression for the spin of the (new) base vectors. To this end, the key equations are:

$$\begin{aligned} w_{l2} &= \mathbf{e}_3^{\mathrm{T}} \mathbf{x}_{21} = 0 \\ w_{l3} &= \mathbf{e}_3^{\mathrm{T}} \mathbf{x}_{31} = 0 \\ \Omega_{lm} &= \left(\frac{\partial u}{\partial \mathbf{Y}} - \frac{\partial v}{\partial \mathbf{X}}\right)_l = 0 \end{aligned} \tag{36}$$

The first two of the above equations (which are consistent with (8) having noted that $Z_1 = Z_2 = Z_3 = 0$) ensure that the local base frame always passes through nodes 2 and 3 (as well as the origin at node 1). Differentiation of the first two of these equations leads to:

$$\mathbf{e}_3^{\mathrm{T}}\delta\mathbf{d}_{21} - \mathbf{x}_{21}^{\mathrm{T}}(\mathbf{S}(\mathbf{e}_3)\delta\boldsymbol{\beta}) = 0$$

$$\mathbf{e}_3^{\mathrm{T}}\delta\mathbf{d}_{31} - \mathbf{x}_{31}^{\mathrm{T}}(\mathbf{S}(\mathbf{e}_3)\delta\boldsymbol{\beta}) = 0 \tag{37}$$

while differentiation of the last equation gives:

$$\delta\Omega_l = \sum \mathbf{a}_l^{j\mathrm{T}}\delta\mathbf{d}_l^j = 0 \tag{38}$$

where $\mathbf{a}_l^j$ and $\delta\mathbf{d}_l^j$ are here of dimension 2×1. (Equation (38) is the two-dimensional equivalent of (21).) With the aid of (19) we can obtain:

$$\delta\mathbf{d}_l^j = \begin{pmatrix}\mathbf{e}_1^{\mathrm{T}}\delta\mathbf{d}^j\\ \mathbf{e}_2^{\mathrm{T}}\delta\mathbf{d}^j\end{pmatrix} + \begin{pmatrix}\mathbf{e}_1^{\mathrm{T}}\mathbf{S}(\mathbf{x}^{j1})\delta\boldsymbol{\beta}\\ \mathbf{e}_2^{\mathrm{T}}\mathbf{S}(\mathbf{x}^{j1})\delta\boldsymbol{\beta}\end{pmatrix} \tag{39}$$

The combination of (38) and (39) provides one equation in the three unknown coefficients of $\delta\boldsymbol{\beta}$ while the two other equations are provided by (37). Hence we can use a similar procedure to that leading to (22) to obtain a relationship of the form:

$$\delta\boldsymbol{\beta} = \mathbf{V}^{\mathrm{T}}\delta\mathbf{p}_t \tag{40}$$

where, for the current three noded triangle, $\mathbf{V}^{\mathrm{T}}$ is of dimensions 3×9 and $\delta\mathbf{p}_t$ contains the changes in the translational global variables.

It is useful to firstly consider the formulation for a curved membrane so that initially we will omit any rotational variables and our element will only have nine translational variables. The transformation matrix $\mathbf{T}$ now takes precisely the same form as that previously given in (23) (although $\mathbf{T}$ is now of dimensions 9×9) while (24) again defines the global internal force vector and (31) defines the initial stress matrix.

We will now turn to the rotational variables. Figure 4 shows a typical surface triad, $\mathbf{U}_s$, as well as the previously discussed element triad, $\mathbf{E}$ (drawn in relation to separate elements purely to avoid cluttering). Let us assume that these triads relate to the initial configuration and can therefore be found from the initial geometry of the shell. As a first stage, for each element, we conceptually relate these nodal triads to the element frame so that:

$$\mathbf{U}_e = [\mathbf{E}\mathbf{U}_s^{\mathrm{T}}]\mathbf{U}_s = \mathbf{X}\mathbf{U}_s \tag{41}$$

and hence in the initial configuration, $\mathbf{U}_e$ is simply $\mathbf{E}$. In the deformed configuration, we would again have:

$$\mathbf{U}_e = \mathbf{X}\mathbf{U}_s \tag{42}$$

where $\mathbf{X}$ is fixed and computed for the original configuration from $\mathbf{U}_e = \mathbf{E}\mathbf{U}_s^{\mathrm{T}}$. In the deformed configuration, of course, $\mathbf{U}_e$ will not (as in the original configuration) coincide with the element $\mathbf{E}$ frame.

The membrane contribution to the element has already been described as has the procedure for choosing the current $\mathbf{E}$ frame. Given some iterative pseudo-vector change $\delta\alpha^j$ at node j (say, from the structural Newton-Raphson iterations), we can up-date $\mathbf{U}_s$ (Fig. 4) according to:

$$\mathbf{U}_{snew} = \mathbf{R}(\delta\alpha)\mathbf{U}_{sold} \tag{43}$$

with $\mathbf{R}(\delta\alpha)$ being computed from Rodriguez formula (Argyris (1982), Crisfield (1990), Nour-Omid *et al.* (1991)). Given the new $\mathbf{U}_s$, the new $\mathbf{U}_e$ can be computed from (42) and we can now obtain the local rotations, θ_l (at the particular node) so that assuming θ_l are reasonably small (Crisfield (to be published), Rankin *et al.* (1986)):

$$\mathbf{S}(\theta_l) = \frac{\mathbf{E}^{\mathrm{T}}\mathbf{U}_e - \mathbf{U}_e^{\mathrm{T}}\mathbf{E}}{2} \tag{44}$$

In the following, we will drop the subscript e on $\mathbf{U}$ (and its components) but the subscript will be implied so that from (44) we can obtain:

$$2\theta_l^j = \begin{bmatrix} \mathbf{e}_3^{\mathrm{T}}\mathbf{u}_2 - \mathbf{u}_3^{\mathrm{T}}\mathbf{e}_2 \\ \mathbf{e}_1^{\mathrm{T}}\mathbf{u}_3 - \mathbf{u}_1^{\mathrm{T}}\mathbf{e}_3 \\ \mathbf{e}_2^{\mathrm{T}}\mathbf{u}_1 - \mathbf{u}_2^{\mathrm{T}}\mathbf{e}_1 \end{bmatrix}^j \tag{45}$$

For the virtual work, we will require the variation of (45) which gives:

$$2\delta\theta_l^j = \mathbf{E}^* \operatorname{col}\mathbf{S}(\mathbf{u}_k)^j \delta\alpha^j - \mathbf{U}^{*j} \operatorname{col}\mathbf{S}(\mathbf{e}_k)\mathbf{V}^{\mathrm{T}}\delta\mathbf{p}_t \tag{46}$$

where $\mathbf{p}_t$ contains the translational nodal variables and:

$$\mathbf{E}^* = \begin{bmatrix} \mathbf{0}^{\mathrm{T}} & -\mathbf{e}_3^{\mathrm{T}} & \mathbf{e}_2^{\mathrm{T}} \\ \mathbf{e}_3^{\mathrm{T}} & \mathbf{0}^{\mathrm{T}} & -\mathbf{e}_1^{\mathrm{T}} \\ -\mathbf{e}_2^{\mathrm{T}} & \mathbf{e}_1^{\mathrm{T}} & \mathbf{0}^{\mathrm{T}} \end{bmatrix}$$

$$\mathbf{U}^{*j} = \begin{bmatrix} \mathbf{0}^{\mathrm{T}} & -\mathbf{u}_3^{\mathrm{T}} & \mathbf{u}_2^{\mathrm{T}} \\ \mathbf{u}_3^{\mathrm{T}} & \mathbf{0}^{\mathrm{T}} & -\mathbf{u}_1^{\mathrm{T}} \\ -\mathbf{u}_2^{\mathrm{T}} & \mathbf{u}_1^{\mathrm{T}} & \mathbf{0}^{\mathrm{T}} \end{bmatrix}^j \tag{47}$$

while:

$$\operatorname{col}\mathbf{S}(\mathbf{e}_k) = \begin{bmatrix} \mathbf{S}(\mathbf{e}_1) \\ \mathbf{S}(\mathbf{e}_2) \\ \mathbf{S}(\mathbf{e}_3) \end{bmatrix}; \quad \operatorname{col}\mathbf{S}(\mathbf{u}_k)^j = \begin{bmatrix} \mathbf{S}(\mathbf{u}_1) \\ \mathbf{S}(\mathbf{u}_2) \\ \mathbf{S}(\mathbf{u}_3) \end{bmatrix}^j \tag{48}$$

The part of the global internal force vector stemming from the "rotational local forces", $\mathbf{q}_{lir}$ is now obtained via the usual equivalence of virtual work in the two systems. Once this process is combined with the similar procedure for the translational internal forces, $\mathbf{q}_{lit}$, (previously just $\mathbf{q}_{li}$ in (24)), we obtain:

$$\begin{aligned} \mathbf{q}_{it} &= \operatorname{col}(\mathbf{E}\mathbf{q}_{lit}^j) - \mathbf{V}\left(\sum_j \left(\mathbf{S}(\mathbf{x}^{j1})\bar{\mathbf{q}}_{lit}^j - \frac{1}{2}(\operatorname{row}\mathbf{S}(\mathbf{e}_k)\mathbf{U}^{*j\mathrm{T}}\mathbf{q}_{lir}^j)\right)\right) \\ &= \operatorname{col}(\bar{\mathbf{q}}_{lit}^j) - \mathbf{V}\left(\sum_j \left(\mathbf{S}(\mathbf{x}^{j1})\bar{\mathbf{q}}_{lit}^j - \frac{1}{2}(\operatorname{row}\mathbf{S}(\mathbf{e}_k)\mathbf{U}^{*j\mathrm{T}}\mathbf{q}_{lir}^j)\right)\right) \end{aligned} \tag{49}$$

Here, the first two terms are taken directly from (24) while the last term stems from the local rotational virtual work:

$$\mathbf{V}_r = \sum \mathbf{q}_{lir}^{jT} \delta\theta_l^j \tag{50}$$

As in the previous developments, the terms following the **V** vector represent three rotational equilibrium equations for the element and will therefore vanish at equilibrium.

Stemming from (5) and the first term in (46), we have global "rotational forces" at each node j of the form:

$$\mathbf{q}_{ir}^j = -\frac{1}{2}\text{row}\,\mathbf{S}(\mathbf{u}_k)^j \mathbf{E}^{*T} \mathbf{q}_{lir}^j = -\frac{1}{2}\text{row}\,\mathbf{S}(\mathbf{u}_k)^j \begin{bmatrix} \mathbf{q}_{lir1}^e \\ \mathbf{q}_{lir2}^e \\ \mathbf{q}_{lir3}^e \end{bmatrix}^j \tag{51}$$

For the initial stress part of the tangent stiffness matrix, the translational-translational terms due to $\mathbf{q}_{lit}$ have already been given in (27) (where the current $\mathbf{q}_{lit}$ were simply $\mathbf{q}_{li}$). From (49), we now have an additional contribution stemming from:

$$\text{Term} = \frac{1}{2}\mathbf{V}\sum_j (\text{row}\,\mathbf{S}(\delta\mathbf{e}_k)\mathbf{U}^{*jT}\mathbf{q}_{lir}^j) = \frac{1}{2}\mathbf{V}\sum_j \left[\text{row}\,\mathbf{S}(\delta\mathbf{e}_k) \begin{bmatrix} \mathbf{q}_{lir1}^u \\ \mathbf{q}_{lir2}^u \\ \mathbf{q}_{lir3}^u \end{bmatrix}^j \right] \tag{52}$$

which gives an additional contribution of the form:

$$\mathbf{K}_{t\sigma}(t,t) = \frac{1}{2}\mathbf{V}\sum_j\sum_k \mathbf{S}(\mathbf{q}_{lirk}^{uj})\mathbf{S}(\mathbf{e}_k)\mathbf{V}^T \tag{53}$$

This term can be combined with the last term in (27) to give a contribution in the form $\mathbf{VZV}^T$ where following previous arguments, the Z term may be symmetrised because it will become symmetric at equilibrium when the term following the matrix **V** in (49) vanishes.

For the term coupling the translational and rotational variables, the variation of (49) leads to a term:

$$\text{Term} = \frac{1}{2}\mathbf{V}\left(\sum_j (\text{row}\,\mathbf{S}(\mathbf{e}_k)\delta\mathbf{U}^{*jT}\mathbf{q}_{lir}^j)\right) \tag{54}$$

which in turn leads to a contribution coupling the translational forces to the rotational variables at node j of the form:

$$\mathbf{K}_{t\sigma}(t,\alpha^j) = \frac{1}{2}\mathbf{V}\,\text{row}\,\mathbf{S}(\mathbf{e}_k) \begin{bmatrix} -\mathbf{q}_{lir}(2)\mathbf{S}(\mathbf{u}_3) & +\mathbf{q}_{lir}(3)\mathbf{S}(\mathbf{u}_2) \\ \mathbf{q}_{lir}(1)\mathbf{S}(\mathbf{u}_3) & -\mathbf{q}_{lir}(3)\mathbf{S}(\mathbf{u}_1) \\ -\mathbf{q}_{lir}(1)\mathbf{S}(\mathbf{u}_2) & +\mathbf{q}_{lir}(2)\mathbf{S}(\mathbf{u}_1) \end{bmatrix}^j \tag{55}$$

From the term involving the variation of (51) with:

$$\text{Term} = -\tfrac{1}{2}\text{row}\,\mathbf{S}(\mathbf{u}_k)\delta\mathbf{E}^{*T}\mathbf{q}_{lir}^j \tag{56}$$

we obtain:

$$\mathbf{K}_{t\sigma}(\alpha^j, t) = -\frac{1}{2}\text{row}\,\mathbf{S}(\mathbf{u}_k)\begin{bmatrix} -\mathbf{q}_{lir}(2)\mathbf{S}(\mathbf{e}_3) & +\mathbf{q}_{lir}(3)\mathbf{S}(\mathbf{e}_2) \\ \mathbf{q}_{lir}(1)\mathbf{S}(\mathbf{e}_3) & -\mathbf{q}_{lir}(3)\mathbf{S}(\mathbf{e}_1) \\ -\mathbf{q}_{lir}(1)\mathbf{S}(\mathbf{e}_2) & +\mathbf{q}_{lir}(2)\mathbf{S}(\mathbf{e}_1) \end{bmatrix}^j \mathbf{V}^{\mathrm{T}} \tag{57}$$

which can be shown to be the transpose of (55).

Finally, the rotational-rotational terms are obtained from the term involving the variation of (51) with:

$$\text{Term} = -\frac{1}{2}\text{row}\,\mathbf{S}(\delta\mathbf{u}_k)^j\mathbf{E}^{*\mathrm{T}}\mathbf{q}^j_{lir} = -\frac{1}{2}\text{row}\,\mathbf{S}(\delta\mathbf{u}_k)^j\begin{bmatrix} \mathbf{q}^e_{lir1} \\ \mathbf{q}^e_{lir2} \\ \mathbf{q}^e_{lir3} \end{bmatrix}^j \tag{58}$$

from which we obtain:

$$\mathbf{K}_{t\sigma}(\alpha^j, \alpha^j) = -\frac{1}{2}\sum_k \mathbf{S}(\mathbf{q}^e_{lirk})^j\mathbf{S}(\mathbf{u}_k)^j \tag{59}$$

This 3×3 sub matrix is in general non-symmetric. However (for conservative loadings), we can probably justify taking the symmetric part by again resorting to the argument of a recovery of symmetry at equilibrium. However, a proof of such a contention would now be more complex as it would involve equilibrium with terms such as (51) now being summed over the element contributions to a particular node. In relation to some beam elements, a similar argument shows that symmetry is almost recovered at equilibrium (Crisfield (to be published)) and that quadratic convergence still results despite the articiical symmetrisation (see also Crisfield (1990)). The elimination of the anti-symmetric terms can also be justified by the use of alternative rotation variables instead of the current "spin quantities, $\delta\alpha$" (Crisfield (to be published)).

A QUADRILATERAL SHELL FORMULATION WITH THREE ROTATIONS PER NODE

Figure 6 illustrates the procedure proposed by Rankin *et al.* (1986) for obtaining a close fit to the curved surface. Again as a starting point, the initial $\mathbf{e}_1$ vector is chosen to lie (as closely as possible along a side). Hence the initial choice of base vectors is:

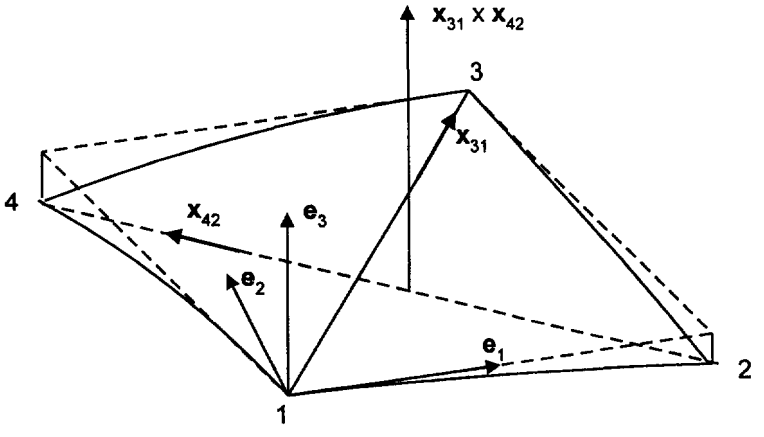

Fig. 6. First choice element frame for a curved quadrilateral.

$$\mathbf{e}_3 = \frac{\mathbf{x}_{13} \times \mathbf{x}_{24}}{\| \mathbf{x}_{13} \| \| \mathbf{x}_{24} \|}; \quad \mathbf{e}_1 = \frac{\mathbf{x}_{21} - (\mathbf{x}_{21}^{\mathrm{T}} \mathbf{e}_3)\mathbf{e}_3}{\| \mathbf{x}_{21} - (\mathbf{x}_{21}^{\mathrm{T}} \mathbf{e}_3)\mathbf{e}_3 \|}; \quad \mathbf{e}_2 = \mathbf{e}_3 \times \mathbf{e}_1 \tag{60}$$

As with the triangular element, a two stage procedure is again applied with the second stage involving eqn (33)–(35) (although we should now emphasise that the subscript l terms are really subscript lm, i.e., they are computed at the centroid of the element).

To obtain the current 3×12 spin matrix $\mathbf{V}^{\mathrm{T}}$, we again use the combination of (38) and (39) for one of the equations in the three components of $\delta\boldsymbol{\beta}$. For the other two, we firstly differentiate (60a) to obtain an equation of the form:

$$\delta \mathbf{e}_3 = \mathbf{A} \delta \mathbf{p} \tag{61}$$

where $\mathbf{A}$ is of dimension 3×12. However, we also know that:

$$\delta \mathbf{e}_3 = -\mathbf{S}(\mathbf{e}_3) \delta \boldsymbol{\beta} \tag{62}$$

so that:

$$\mathbf{e}_1^{\mathrm{T}} \mathbf{A} \delta \mathbf{p} = -\mathbf{e}_1^{\mathrm{T}} \mathbf{S}(\mathbf{e}_3) \delta \boldsymbol{\beta} = \mathbf{e}_2^{\mathrm{T}} \delta \boldsymbol{\beta}$$

and

$$\mathbf{e}_2^{\mathrm{T}} \mathbf{A} \delta \mathbf{p} = -\mathbf{e}_2^{\mathrm{T}} \mathbf{S}(\mathbf{e}_3) \delta \boldsymbol{\beta} = -\mathbf{e}_1^{\mathrm{T}} \delta \boldsymbol{\beta} \tag{63}$$

provide the remaining two equations from which we can obtain (40) with $\mathbf{V}^{\mathrm{T}}$ now being of dimension 3×12. Apart from the different nature of the $\mathbf{V}$ matrix and the different number of nodes, the formation of the internal force vector and tangent stiffness matrix takes essentially the same form as it did for the three-noded triangle.

There is no reason why the element level computations should be restricted to a facet. They could instead involve a shallow shell formulation. In these circumstances, it would be necessary to revise the procedure discussed at the beginning of this section to set up the element nodel frame, $\mathbf{U}_e$, from the surface nodal frame $\mathbf{U}_s$. Instead we could obtain the initial value of the $\mathbf{U}_e$ frame by rotating the initial element $\mathbf{E}$ frame through the vector angle, γ between $\mathbf{e}_3$ and $\mathbf{u}_{s3}$ where:

$$\gamma = \cos^{-1}(\mathbf{e}_3^{\mathrm{T}} \mathbf{u}_{s3}) \frac{\mathbf{e}_3 \mathbf{x} \mathbf{u}_{s3}}{\| \mathbf{e}_3 \mathbf{x} \mathbf{u}_{s3} \|} \tag{64}$$

so that initially

$$\mathbf{U}_e = \mathbf{R}(\gamma) \mathbf{E} \tag{65}$$

with $\mathbf{R}(\gamma)$ being obtained via the Rodriguez formula (Argyris (1982), Crisfield (1990), Nour-Omid *et al.* (1991)). The initial local rotations could then be computed from (45). In addition, the matrix $\mathbf{X}$ of (42) could be computed in the initial configuration as $\mathbf{X} = \mathbf{U}_e \mathbf{U}_s^{\mathrm{T}}$ and subsequently used in the current configuration in conjunction with (42) to obtain $\mathbf{U}_e$ from $\mathbf{U}_s$. It is worth re-emphasising that from (45) onwards, the expressions for $\mathbf{U}$ have an implied subscript e (see the text below (44)). It is also worth mentioning that the formulation at the local element level can itself be non-linear (Crisfield (to be published)).

A SHELL FORMULATION WITH TWO ROTATIONAL DEGREES-OF-FREEDOM PER NODE

As discussed in the introduction, the previous formulations have some serious drawbacks because of the need for a drilling rotation at the local element level. As an alternative,

two rotational variables could be used for those nodes associated with a smooth part of the shell while three rotational variables (using the previous procedure) could be used for those nodes associated with a branched junction.

Let us assume that in the initial configuration, we know the unit normal surface vector $\mathbf{u}_3$ (Fig. 4) as well as the element triad $\mathbf{E} = [\mathbf{e}_1, \mathbf{e}_2, \mathbf{e}_3]$. In which case we can approximate the initial local rotations as:

$$\theta_{l2} = -\mathbf{u}_3^{\mathrm{T}}\mathbf{e}_2\,; \quad \theta_{l1} = \mathbf{u}_3^{\mathrm{T}}\mathbf{e}_1 \tag{66}$$

The directions $\mathbf{u}_1$ and $\mathbf{u}_2$ can be arbitrarily chosen with, say, $\mathbf{u}_2$ lying above a particular side. For a first load increment, we will keep this surface triad fixed as $\mathbf{U}_o$ (subscript o for old) and will allow two rotations α_1 about $\mathbf{u}_{1o}$ and α_2 about $\mathbf{u}_{2o}$. We will now be concerned with the up-dating, within the increment, of $\mathbf{u}_{3o}$ to $\mathbf{u}_{3n}$ (subscript n for new). To this end we will operate in fixed surface co-ordinates (with components along $\mathbf{u}_{1o}$, $\mathbf{u}_{2o}$ and $\mathbf{u}_{3o}$). We will use a superimposed bar to denote that quantities are written with respect to these axes. Then we have:

$$\bar{\mathbf{u}}_{3o} = \begin{bmatrix} 0 \\ 0 \\ 1 \end{bmatrix} \tag{67}$$

and (see Fig. 7):

$$\bar{\mathbf{u}}_{3n} = \cos\alpha\,\bar{\mathbf{u}}_{3o} + \frac{\sin\alpha}{\alpha}\boldsymbol{\alpha} \times \bar{\mathbf{u}}_{3o} \tag{68}$$

where:

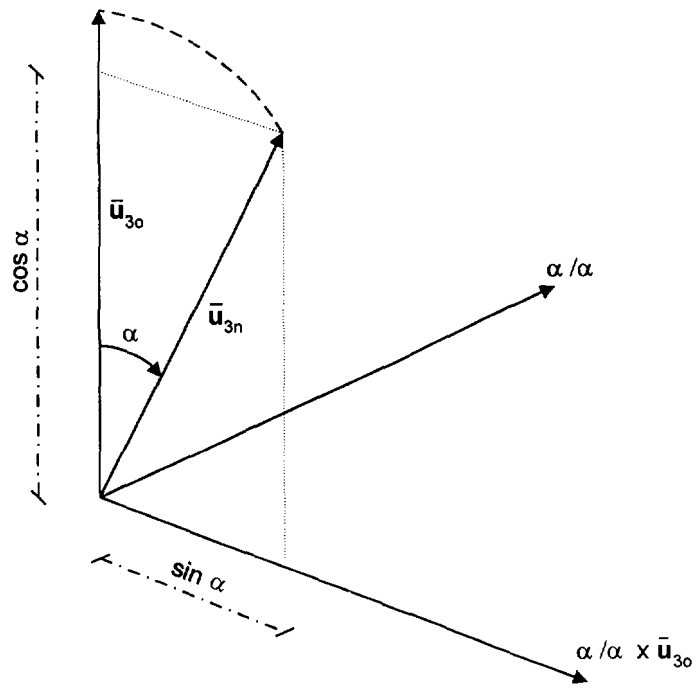

Fig. 7. Rotating $\bar{\mathbf{u}}_{3o}$ to $\bar{\mathbf{u}}_{3n}$.

$$\alpha^T = (\alpha_1, \alpha_2, 0); \quad \alpha = (\alpha_1^2 + \alpha_2^2)^{1/2} \tag{69}$$

With respect to the usual fixed cartesian co-ordinate frame, we can then compute:

$$\mathbf{u}_{3n} = \mathbf{U}_o \bar{\mathbf{u}}_{3n} \tag{70}$$

with the current local rotations then being obtained in a similar fashion to (66) i.e. with:

$$\theta_{l2} = -\mathbf{u}_{3n}^T \mathbf{e}_2; \quad \theta_{l1} = \mathbf{u}_{3n}^T \mathbf{e}_1 \tag{71}$$

where $\mathbf{e}_1$ and $\mathbf{e}_2$ now relate to the current (new) element frame. At this stage we have all the required local quantities to pass to the local element routines so as to compute $\mathbf{q}_{lit}$ and $\mathbf{q}_{lir}$ where, for a simple triangle, the latter will be of dimensions six.

With a view to the virtual work, we can write:

$$\delta \bar{\mathbf{u}}_{3n} = \delta\alpha \times \bar{\mathbf{u}}_{3n} = -\mathbf{S}^*(\bar{\mathbf{u}}_{3n}) \delta\alpha_2 \tag{72}$$

where we have introduced the * on S to indicate that the current matrix is of dimensions 3×2, i.e.:

$$\mathbf{S}^*(\mathbf{a}) = \begin{bmatrix} 0 & -a_3 \\ a_3 & 0 \\ -a_2 & a_1 \end{bmatrix} \tag{73}$$

and the subscript 2 on $\delta\alpha$ implies that we have only two components, $\delta\alpha_1$ and $\delta\alpha_2$. For the future developments, we will drop this subscript on $\delta\alpha$ (and on α) which will be assumed to be of dimensions 2×1.

Using (70) and (72), we can obtain the variation of (71) as:

$$\delta\theta_{l1} = \mathbf{u}_{3n}^T \mathbf{S}(\mathbf{e}_2) \delta\boldsymbol{\beta} + \mathbf{e}_2^T \mathbf{U}_o \mathbf{S}^*(\bar{\mathbf{u}}_{3n}) \delta\alpha \tag{74a}$$

$$\delta\theta_{l2} = -\mathbf{u}_{3n}^T \mathbf{S}(\mathbf{e}_1) \delta\boldsymbol{\beta} - \mathbf{e}_1^T \mathbf{U}_o \mathbf{S}^*(\bar{\mathbf{u}}_{3n}) \delta\alpha \tag{74b}$$

so that, in conjunction with the relationships of (40) and (24), we can construct the element **T** matrix and hence obtain the internal force vector for which the translational terms may be explicitly written as:

$$\mathbf{q}_{it} = \text{col}(\bar{\mathbf{q}}_{lit}^j) - \mathbf{V}\left(\sum_j (\mathbf{S}(\mathbf{x}^{j1}) \bar{\mathbf{q}}_{lit}^j + \mathbf{S}(\mathbf{e}_2)(\mathbf{q}_{lir}(1)^j \mathbf{u}_{3n}^j) - \mathbf{S}(\mathbf{e}_1)(\mathbf{q}_{lir}(2)^j \mathbf{u}_{3n})) \right) \tag{75}$$

while at node j the rotational terms may be expressed as:

$$\mathbf{q}_{ir}^j = \mathbf{q}_{lir}(1) \mathbf{S}^*(\bar{\mathbf{u}}_{3n})^T \mathbf{U}_o^T \mathbf{e}_2 - \mathbf{q}_{lir}(2) \mathbf{S}^*(\bar{\mathbf{u}}_{3n})^T \mathbf{U}_o^T \mathbf{e}_1 \tag{76}$$

where $\mathbf{q}_{ir}^j$ is of dimensions 2×1.

For the initial stress matrix, the translational-translational terms due to $\mathbf{q}_{lit}$ in (75) have already been given in (27) (although the current $\mathbf{q}_{lit}$ were in (27) simply referred to as $\mathbf{q}_{li}$) From (75), we now have an additional contribution stemming from:

$$\text{Term} = -\mathbf{V}\left(\sum_j (\mathbf{S}(\delta\mathbf{e}_2)(\mathbf{q}_{lir}(1)^j \mathbf{u}_{3n}^j) - \mathbf{S}(\delta\mathbf{e}_1)(\mathbf{q}_{lir}(2)^j \mathbf{u}_{3n}^j)) \right) \tag{77}$$

which gives an additional contribution of the form:

$$\mathbf{K}_{t\sigma}(t,t) = \mathbf{V}\sum_j (\mathbf{q}_{lir}(1)^j\mathbf{S}(\mathbf{u}^j_{3n})\mathbf{S}(\mathbf{e}_2) - \mathbf{q}_{lir}(2)^j\mathbf{S}(\mathbf{u}^j_{3n})\mathbf{S}(\mathbf{e}_1))\mathbf{V}^{\mathrm{T}} \tag{78}$$

Also stemming from (75), we have a translational coupling term stemming from:

$$\text{Term} = -\mathbf{V}\left(\sum_j (\mathbf{S}(\mathbf{e}_2)(\mathbf{q}_{lir}(1)^j\delta\mathbf{u}^j_{3n}) - \mathbf{S}(\delta\mathbf{e}_1)(\mathbf{q}_{lir}(2)^j\delta\mathbf{u}^j_{3n}))\right) \tag{79}$$

which leads to a term coupling the translational forces to the rotational variables at node j of the form:

$$\mathbf{K}_{t\sigma}(t,\alpha^j) = \mathbf{V}(-\mathbf{q}_{lir}(1)^j\mathbf{S}(\mathbf{e}_2)\mathbf{U}^j_o\mathbf{S}^*(\bar{\mathbf{u}}^j_{3n}) + \mathbf{q}_{lir}(2)^j\mathbf{S}(\mathbf{e}_1)\mathbf{U}^j_o\mathbf{S}^*(\bar{\mathbf{u}}^j_{3n})) \tag{80}$$

The transpose of the above is obtained from the variation of the terms $\mathbf{e}_1$ and $\mathbf{e}_2$ in (76) while also from (76) we obtain a rotational-rotational term:

$$\begin{aligned}\text{Term} &= \mathbf{q}_{lir}(1)\mathbf{S}^*(\delta\bar{\mathbf{u}}_{3n})^{\mathrm{T}}\mathbf{U}_o^{\mathrm{T}}\mathbf{e}_2 - \mathbf{q}_{lir}(2)\mathbf{S}^*(\delta\bar{\mathbf{u}}_{3n})^{\mathrm{T}}\mathbf{U}_o^{\mathrm{T}}\mathbf{e}_1 \\ &= \mathbf{q}_{lir}(1)\mathbf{S}^*(\delta\bar{\mathbf{u}}_{3n})^{\mathrm{T}}\mathbf{e}_2^u - \mathbf{q}_{lir}(2)\mathbf{S}^*(\delta\bar{\mathbf{u}}_{3n})^{\mathrm{T}}\mathbf{e}_1^u\end{aligned} \tag{81}$$

where we have introduced the vectors $\mathbf{e}_1^u = \mathbf{U}_o^{\mathrm{T}}\mathbf{e}_1$ and $\mathbf{e}_2^u = \mathbf{U}_o^{\mathrm{T}}\mathbf{e}_2$ so that we can evaluate (81) as leading to:

$$\mathbf{K}_{t\sigma}(\alpha^j,\alpha^j) = \mathbf{q}_{lir}(1)\mathbf{S}^*(\mathbf{e}_2^u)^{\mathrm{T}}\mathbf{S}^*(\bar{\mathbf{u}}_{3n}) - \mathbf{q}_{lir}(2)\mathbf{S}^*(\mathbf{e}_1^u)^{\mathrm{T}}\mathbf{S}^*(\bar{\mathbf{u}}_{3n}) \tag{82}$$

Following the previous arguments, we believe that (for conservative loadings), an artificial symmetrisation of the terms in (78) and (82) will again produce a formulation with good convergence characteristics. However, numerical experiments are required.

A FACET SHELL FORMULATION BASED ON MORLEY'S TRIANGLE

As discussed in the Introduction, an alternative for avoiding the drilling rotation is to use a rotation about an element side as originally applied in a linear context by Herrmann (1968) and in relation to a displacement formulation by Morley (1971). The element was later used for non-linear shells by Backlund (1973) and Chen (1979). In contrast to these shell formulations, the first authors' co-rotational approach included a consistent linearisation and was not step-size dependant (Peng and Crisfield (1992)). However, the formulation was rather complex and the aim of the present development is to use the current general framework to reduce this complexity.

The element frame and equivalent spin matrix, $\mathbf{V}^{\mathrm{T}}$ can be taken to be identical to that for the triangular shell that has already been discussed. For the mid-side rotational variables, we will suppose a current triad composed of $\mathbf{r}_1$, $\mathbf{r}_2$ and $\mathbf{r}_3$ (Fig. 8(c)) with $\mathbf{r}_2$ lying along a side with node j at the "front" of $\mathbf{r}_2$ and node i at the "tail". For a simple facet formulation, the initial side triad $\mathbf{R}_1$, $\mathbf{R}_2$ and $\mathbf{R}_3$ can be found with $\mathbf{R}_3$ coinciding with the initial value of $\mathbf{e}_3$ (i.e. being perpendicular to the plane of the initial facet). To obtain the equivalent current triad, we firstly obtain $\mathbf{r}_2$ from:

$$\mathbf{r}_2 = \frac{\mathbf{x}_{ji}}{\|\mathbf{x}_{ji}\|} \tag{83}$$

and then rotate the initial triad $\mathbf{R}_1$–$\mathbf{R}_3$ in the plane formed by $\mathbf{R}_2$ and $\mathbf{r}_2$ through the vector angle:

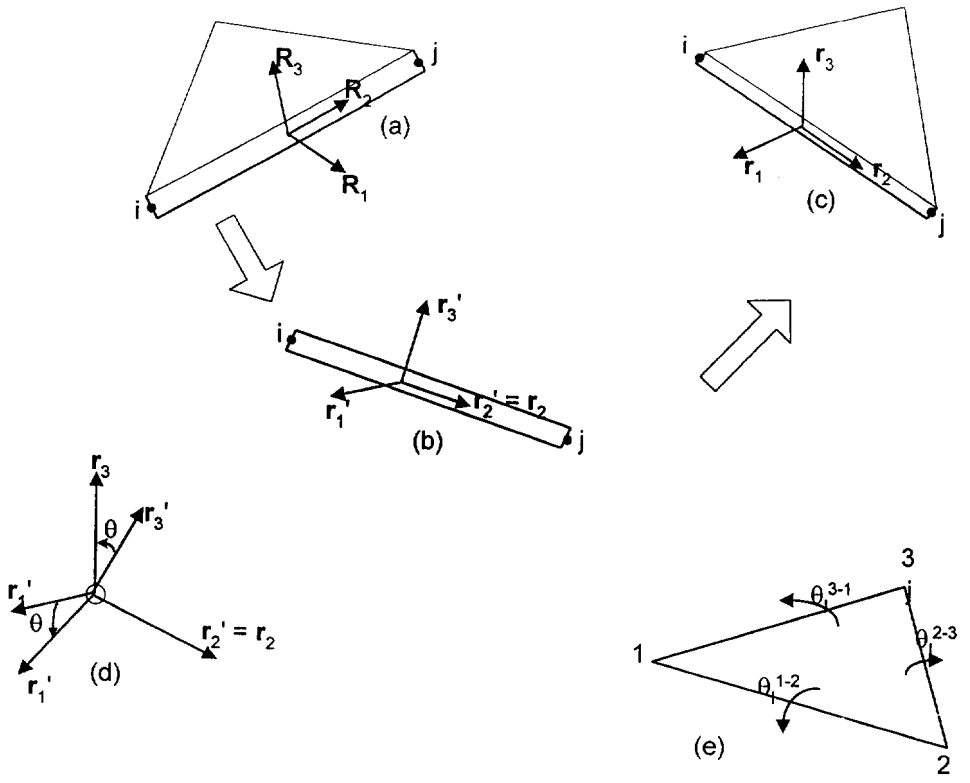

Fig. 8. Rotational variables and triads for use with Morley's triangle (a) initial mid-side triad $[\mathbf{R}_1, \mathbf{R}_2, \mathbf{R}_3]$ for side *ji* (initial configuration), (b) intermediate mid-side triad $[\mathbf{r}'_1, \mathbf{r}'_2, \mathbf{r}'_3]$ in current configuration, (c) final mid-side triad in current configuration, (d) global mid-side rotation, θ, (e) local mid-side rotations θ_i.

$$\gamma = -\cos^{-1}(\mathbf{R}_2^{\mathrm{T}}\mathbf{r}_2)\frac{\mathbf{R}_2 \mathbf{x} \mathbf{r}_2}{\| \mathbf{R}_2 \mathbf{x} \mathbf{r}_2 \|} \tag{84}$$

As a result of this exercise, the initial mid-side triad $\mathbf{R}_1$–$\mathbf{R}_3$ becomes the triad $\mathbf{r}'_1$–$\mathbf{r}'_3$ (Fig. 8b) where $\mathbf{r}'_2 = \mathbf{r}_2$ but, in general, $\mathbf{r}'_1 \neq \mathbf{r}_1$ and $\mathbf{r}'_3 \neq \mathbf{r}_3$. In order to reach the final configuration with the mid-side triad of $\mathbf{r}_1$–$\mathbf{r}_3$, we now apply the (positive clockwise) global rotation, θ, about the $\mathbf{r}_2 = \mathbf{r}'_2$ axis. This leads to the relationships:

$$\mathbf{r}_1 = \mathbf{r}'_1 \cos\theta - \mathbf{r}'_3 \sin\theta \tag{85a}$$

$$\mathbf{r}_2 = \mathbf{r}'_2 \tag{85b}$$

$$\mathbf{r}_3 = \mathbf{r}'_1 \sin\theta + \mathbf{r}'_3 \cos\theta \tag{85c}$$

Having computed the triad, $\mathbf{r}_1$–$\mathbf{r}_3$, the current (clockwise) local mid-side rotations (Fig. 8e) can be obtained using:

$$\sin\theta_i = -\mathbf{e}_3^{\mathrm{T}}\mathbf{r}_1 \tag{86}$$

At this stage, we should note that the $\mathbf{r}'$ triad can be computed from:

$$[\mathbf{r}'_1, \mathbf{r}'_2, \mathbf{r}'_3] = \mathbf{R}(\gamma)[\mathbf{R}_1, \mathbf{R}_2, \mathbf{R}_3] \tag{87}$$

where $\mathbf{R}(\gamma)$ is obtained from the Rodriguez formula (Argyris (1982), Crisfield (1990), Nour-Omid *et al.* (1991)) or as an alternative equivalent from:

$$\mathbf{r}_1' = \mathbf{R}_1 - \frac{b_1}{1+b_2}(\mathbf{R}_2 + \mathbf{r}_2) \tag{88a}$$

$$\mathbf{r}_2' = \mathbf{r}_2 \tag{88b}$$

$$\mathbf{r}_3' = \mathbf{R}_3 - \frac{b_3}{1+b_2}(\mathbf{R}_2 + \mathbf{r}_2) \tag{88c}$$

where:

$$b_k = \mathbf{R}_k^T \mathbf{r}_2 = -\mathbf{r}_k'^T \mathbf{R}_2 \tag{89}$$

With a view to the use of virtual work, we require the variation of (86) so that:

$$\delta\theta_l = \frac{-1}{\cos\theta_l}(\mathbf{e}_3^T \delta\mathbf{r}_1 + \delta\mathbf{e}_3^T \mathbf{r}_1) \tag{90}$$

The change in the $\mathbf{e}_3$ vector is simply:

$$\delta\mathbf{e}_3 = -\mathbf{S}(\mathbf{e}_3)\delta\boldsymbol{\beta} = -\mathbf{S}(\mathbf{e}_3)\mathbf{V}^T \delta\mathbf{p}_t \tag{91}$$

where we have used (40) for $\delta\boldsymbol{\beta}$ and $\delta\mathbf{p}_t$ relates to the translational nodal variables. With a view to the insertion of (91) into (90), we also note that:

$$\mathbf{e}_3 \times \mathbf{r}_1 = \mathbf{S}(\mathbf{e}_3)\mathbf{r}_1 = \mathbf{r}_2 \cos\theta_l \tag{92}$$

and hence for the last term in (90), we have:

$$\frac{-1}{\cos\theta_l}(\delta\mathbf{e}_3^T \mathbf{r}_1) = -\mathbf{r}_2^T \delta\boldsymbol{\beta} = -\mathbf{r}_2^T \mathbf{V}^T \delta\mathbf{p}_t \tag{93}$$

With a view to the first term in (90), differentiation of (85a) and (88) leads, after some manipulation, to:

$$\delta\mathbf{r}_1 = \frac{1}{(1+b_2)}[-(\mathbf{R}_2 + \mathbf{r}_2)\mathbf{r}_1^T + (\mathbf{R}_2^T \mathbf{r}_1)\mathbf{I}]\delta\mathbf{r}_2 - \mathbf{r}_3 \delta\theta = \frac{-1}{(1+b_2)}\mathbf{S}(\mathbf{r}_1)\mathbf{S}(\mathbf{R}_2 + \mathbf{r}_2)\delta\mathbf{r}_2 - \mathbf{r}_3 \delta\theta \tag{94}$$

where the scalar b_2 comes from (89). Substitution from (94) and (92) into (90) leads to:

$$\delta\theta_l = \delta\theta - \frac{1}{(1+b_2)}\mathbf{r}_2^T \mathbf{S}(\mathbf{R}_2 + \mathbf{r}_2)\delta\mathbf{r}_2 - \mathbf{r}_2^T \mathbf{V}^T \delta\mathbf{p}_t \tag{95}$$

To proceed further we can either express $\delta\mathbf{r}_2$ via:

$$\delta\mathbf{r}_2 = -\mathbf{S}(\mathbf{r}_2)\delta\boldsymbol{\beta} = -\mathbf{S}(\mathbf{r}_2)\mathbf{V}^T \delta\mathbf{p}_t \tag{96a}$$

or via:

$$\delta\mathbf{r}_2 = \frac{1}{s}[\mathbf{I} - \mathbf{r}_2 \mathbf{r}_2^T]\delta\mathbf{d}_{ji} \tag{96b}$$

where s is the current length of the side along which $\mathbf{r}_2$ lies.

While the former might seem the most direct, it turns out that there are some advantages in using the latter so that substitution into (95) leads to:

$$\delta\theta_l = \delta\theta + \frac{1}{(1+b_2)s}(\mathbf{R}_2 \times \mathbf{r}_2)^{\mathrm{T}}\delta\mathbf{d}_{ji} - \mathbf{r}_2^{\mathrm{T}}\mathbf{V}^{\mathrm{T}}\delta\mathbf{p}_t \tag{97}$$

By equating the virtual work in the local and global systems, we now arrive at the "translational" internal forces as:

$$\mathbf{q}_{it} = \mathrm{col}(\bar{\mathbf{q}}_{lit}^j) - \mathbf{V}\left(\sum_j (\mathbf{S}(\mathbf{x}^{j1})\bar{\mathbf{q}}_{lit}^j) + \sum_k (\mathbf{q}_{lir}^k \mathbf{r}_2^k)\right) + \mathbf{q}_{it}^* \tag{98}$$

where the first two terms are related to local translations and take the same form as in (49) while the last two terms stem from the "rotational local virtual work" via (97). In (98), the sum j is over the corner nodes and the sum k is over the mid-side nodes. For a particular corner node j, the contribution to $\mathbf{q}_{it}^*$ (which stems from the second term in (97)) is:

$$\mathbf{q}_{it}^{*j} = \left(\mathbf{q}_{lir}\frac{1}{(1+b_2)s}(\mathbf{R}_2 \times \mathbf{r}_2)\right)^{j-} - \left(\mathbf{q}_{lir}\frac{1}{(1+b_2)s}(\mathbf{R}_2 \times \mathbf{r}_2)\right)^{j+} \tag{99}$$

where $j-$ is the mid-side node clockwise behind the node and $j+$ is the mid-side node clockwise ahead of the corner node.

For the "rotational internal forces", using (97), the equivalence of virtual work in the local and global systems leads to the trivial relationship:

$$\mathbf{q}_{ir} = \mathbf{q}_{lir} \tag{100}$$

at each of the mid-side nodes.

It is now useful to study the equilibrium relationships in (98) and (99). As in the previous developments, the terms following the $\mathbf{V}$ matrix in (98) can be identified as three rotational equilibrium equations for the element and will therefore vanish at equilibrium. Noting the results in (100), if no external moments are applied, any particular mid-side internal moment will, via (99) contribute terms to the translational forces of an adjacent corner node which will be exactly cancelled by the equivalent contributions from the adjacent element. Hence we can argue that at the structural level the $\mathbf{q}_{it}^*$ terms in (98) and (99) will vanish at equilibrium. We will use these arguments to justify the omission of certain terms in the following derivation of the initial stress matrix, $\mathbf{K}_{t\sigma}$. (It is possible to include all terms (Peng and Crisfield (1992)) but the resulting equations are rather complex.)

The translational-translational terms in $\mathbf{K}_{t\sigma}$ due to $\mathbf{q}_{lit}$ in (98) have already been given in (27) (although the current $\mathbf{q}_{lit}$ were in (27) simply referred to as $\mathbf{q}_{li}$). From (98), we now have an additional contribution stemming from:

$$\text{Term} = -\mathbf{V}\left(\sum_k (\mathbf{q}_{lir}^k \delta\mathbf{r}_2^k)\right) \tag{101}$$

which, using $\delta\mathbf{r}_2$ from (96a) gives an additional contribution of the form:

$$\mathbf{K}_{t\sigma}(t,t) = \mathbf{V}\sum_k (\mathbf{q}_{lir}^k \mathbf{S}(\mathbf{r}_2^k))\mathbf{V}^{\mathrm{T}} \tag{102}$$

When this term is combined with the last term in (27), it can be expressed in the form $\mathbf{V}\mathbf{Z}\mathbf{V}^{\mathrm{T}}$ where following previous arguments, the $\mathbf{Z}$ term may be symmetrised because it will become symmetric at equilibrium when the term following $\mathbf{V}$ in (98) vanishes.

The previous developments have followed the work in Peng and Crisfield (1992) and have used a "total formulation" in which the current mid-side triad $[\mathbf{r}_1, \mathbf{r}_2, \mathbf{r}_3]$ is up-dated directly from the initial triads $[\mathbf{R}_1, \mathbf{R}_2, \mathbf{R}_3]$ via the total global rotation, θ. Numerical experiments have shown that a more robust formulation can be devised by re-setting $\mathbf{R}_{1-3} = \mathbf{r}_{1-3}$ and $\theta = 0$ at the end of each increment. The key equations remain unaltered and, in particular, the local rotations are still computed from (86). Van Keulen *et al.* (1993) go one stage further and apply this up-date at the end of each iteration. As a consequence (with $\mathbf{R}_2 = \mathbf{r}_2$), some of the previous expressions can be simplified further.

Irons' semi-loof shell element (Irons (1976)) can be considered as a higher-order version of the Morley triangle. An outline of a possible extension of the current co-rotational harness in order to incorporate this element described in Crisfield (to be published).

3-D BEAMS

The earlier developments can be used to produce a formulation for three-dimensional beams. The procedure is very similar to that described earlier for a shell element with three rotations at each node although now we have a beam with three two rotations at each node. As with the shell, we will now define the pseudo-vector rotations at node j ($j = 1, 2$) as $\boldsymbol{\alpha}^j$ with the equivalent triad as $\mathbf{U}^j$ while the translations at node j will be $\mathbf{d}^j$ while the local rotations will be θ_l^j.

We now need to define the local **E** frame. To this end the vector $\mathbf{e}_1$ can be very simply defined as the unit vector that in the current configuration lies between nodes 1 and 2, i.e.:

$$\mathbf{e}_1 = \frac{\mathbf{x}_{21}}{\| \mathbf{x}_{21} \|} \tag{103}$$

There are number of options for defining the other two unit vectors $\mathbf{e}_2$ and $\mathbf{e}_3$ (Crisfield (1990), Rankin *et al.* (1986), Nour-Omid *et al.* (1991)). Perhaps the simplest is that described by Rankin *et al.* (1986) and Nour-Omid *et al.* (1991). Using their approach, one firstly relates the nodal triads $\mathbf{U}^1$ and $\mathbf{U}^2$ to the element frame using the same procedure as that discussed earlier for "a triangular shell element with three rotational variables per node", in particular, using the procedure related to the discussion associated with eqns (41) and (42). This technique requires the **E** frame in the initial configuration which is easily defined using the principal directions of inertia.

Given the current nodal triads $\mathbf{U}_e^1$ and $\mathbf{U}_e^2$ and knowing $\mathbf{e}_1$ from (103), using Rankin and Brogan"s technique, the $\mathbf{e}_3$ vector is computed from:

$$\mathbf{e}_3 = \mathbf{e}_1 \times \mathbf{u}_{e2}^1 \tag{104}$$

where $\mathbf{u}_{e2}^1$ is the second column of $\mathbf{U}_e^1$ (at node 1). The vector $\mathbf{e}_2$ is computed so as to make up an orthogonal element triad, i.e. via:

$$\mathbf{e}_2 = -\mathbf{e}_1 \times \mathbf{e}_3 = \mathbf{u}_{e2}^1 - (\mathbf{u}_{e2}^{1\mathrm{T}} \mathbf{e}_1)\mathbf{e}_1 \tag{105}$$

As noted by Rankin *et al.* (1986), this procedure will ensure that rotations about the axis of the beam will remain of the same order as those which produce torsion.

In order to obtain the important spin matrix, $\mathbf{V}^{\mathrm{T}}$, we can first apply the conditions that the local axes pass through the second node so that:

$$\mathbf{v}_{l2} = \mathbf{e}_2^{\mathrm{T}} \mathbf{x}_{21} = 0; \quad \mathbf{w}_{l2} = \mathbf{e}_3^{\mathrm{T}} \mathbf{x}_{21} = 0 \tag{106}$$

differentiation of the above gives:

$$\mathbf{x}_{21}^{\mathrm{T}}\delta\mathbf{e}_2+\mathbf{e}_2^{\mathrm{T}}\delta\mathbf{d}_{21} = -\mathbf{x}_{21}^{\mathrm{T}}\mathbf{S}(\mathbf{e}_2)\delta\boldsymbol{\beta}+\mathbf{e}_2^{\mathrm{T}}\delta\mathbf{d}_{21} = 0 \tag{107}$$

$$\mathbf{x}_{21}^{\mathrm{T}}\delta\mathbf{e}_3+\mathbf{e}_3^{\mathrm{T}}\delta\mathbf{d}_{21} = -\mathbf{x}_{21}^{\mathrm{T}}\mathbf{S}(\mathbf{e}_3)\delta\boldsymbol{\beta}+\mathbf{e}_3^{\mathrm{T}}\delta\mathbf{d}_{21} = 0 \tag{108}$$

Equations (107) and (108) provide two equations in three components of $\delta\boldsymbol{\beta}$. We can now differentiate eqn (106) and pre-multiply by $\mathbf{e}_2^{\mathrm{T}}$ to obtain a third equation:

$$\mathbf{e}_2^{\mathrm{T}}\mathbf{S}(\bar{\mathbf{u}}_2^1)\delta\alpha_1 = -(\bar{\mathbf{u}}_2^{1\mathrm{T}}\mathbf{e}_1)\mathbf{e}_3^{\mathrm{T}}\delta\boldsymbol{\beta} \tag{109}$$

where $\delta\alpha_1$ is the pseudo vector change at the first node. Using eqns (107)–(109), we can obtain the equivalent of (40) whereby:

$$\delta\boldsymbol{\beta} = \mathbf{V}^{\mathrm{T}}\delta\mathbf{p} \tag{110}$$

In contrast to the previous work on shells, $\delta\boldsymbol{\beta}$ is now coupled to the rotational variables and is not just related to the translational variables. (The equivalent formulation using Crisfield's approach (1990) for defining the $\mathbf{e}_2$ and $\mathbf{e}_3$ vectors is described in Crisfield (to be published).)

Having obtained the 3×12 $\mathbf{V}^{\mathrm{T}}$ matrix, we are now in a position to apply a very similar procedure to that of the earlier section on shells. In particular from (19), we would have:

$$\delta\mathbf{d}_l^j = \mathbf{E}^{\mathrm{T}}\delta\mathbf{d}^j+\mathbf{E}^{\mathrm{T}}\mathbf{S}(\mathbf{x}^{j1})\mathbf{V}^{\mathrm{T}}\delta\mathbf{p} \tag{111}$$

while from (46) we would obtain:

$$2\delta\theta_l^j = \mathbf{E}^*\,\mathrm{col}\,\mathbf{S}(\mathbf{u}_k)^j\delta\alpha^j-\mathbf{U}^{*j}\,\mathrm{col}\,\mathbf{S}(\mathbf{e}_k)\mathbf{V}^{\mathrm{T}}\delta\mathbf{p} \tag{112}$$

from which the 12×12 transformation matrix $\mathbf{T}$ can be obtained and hence the global internal force vector. It should be noted that, as in the section on shells, in (112) and in the following equations we have dropped the subscript e on $\mathbf{U}$ and its vector components.

The initial stress matrix would then follow by combining the last part of (27) with (52) to give a contribution:

$$\mathbf{K}_{l\sigma}(\mathbf{p},\mathbf{p}) = \mathbf{V}\left(\sum_j \mathbf{S}(\mathbf{x}^{j1})\mathbf{S}(\bar{\mathbf{q}}_{lit}^j)+\frac{1}{2}\sum_j\sum_k \mathbf{S}(\mathbf{q}_{lirk}^{uj})\mathbf{S}(\mathbf{e}_k)\right)\mathbf{V}^{\mathrm{T}} \tag{113}$$

where following previous arguments, the central part could be symmetrised. Also, from (27) and (55), we would obtain a contribution connecting all of the variables ($\mathbf{p}$) to the pseudo vector rotations at node j ($\boldsymbol{\alpha}^j$) of the form:

$$\mathbf{K}_{l\sigma}(\mathbf{p},\boldsymbol{\alpha}^j) = \mathbf{V}\left[\mathrm{row}(\mathbf{S}(\bar{\mathbf{q}}_{lit}^j))+\tfrac{1}{2}\mathrm{row}\,\mathbf{S}(\mathbf{e}_k)\begin{bmatrix} -\mathbf{q}_{lir}(2)\mathbf{S}(\mathbf{u}_3) & +\mathbf{q}_{lir}(3)\mathbf{S}(\mathbf{u}_2)\\ \mathbf{q}_{lir}(1)\mathbf{S}(\mathbf{u}_3) & -\mathbf{q}_{lir}(3)\mathbf{S}(\mathbf{u}_1)\\ -\mathbf{q}_{lir}(1)\mathbf{S}(\mathbf{u}_2) & +\mathbf{q}_{lir}(2)\mathbf{S}(\mathbf{u}_1)\end{bmatrix}^j\right] \tag{114}$$

with equivalent transposed terms. Finally, from (58) we would obtain the rotation-rotation terms as:

$$\mathbf{K}_{l\sigma}(\boldsymbol{\alpha}^j,\boldsymbol{\alpha}^j) = -\frac{1}{2}\sum_k \mathbf{S}(\mathbf{q}_{lirk}^e)^j\mathbf{S}(\mathbf{u}_k)^j \tag{115}$$

Following previous arguments, we believe that the latter may be symmetrised.

CONCLUSION

The paper has described a general co-rotational framework which is introduced for three-dimensional continuum elements and is later applied to the derivation of the governing equations for applications with beams and shells. In the latter case, the "drilling rotation" may either be directly introduced or alternatively it may be omitted either by using two rotational variables at corner nodes or single rotational variables at nodes along the sides. The adopted procedure automatically indicates certain terms that may be neglected in the generation of the tangent stiffness matrix because they will vanish (or almost vanish) at equilibrium. While the work with continuum elements has been backed by numerical computations that are described in other papers, the work on beams and shells has yet to be numerically tested in relation to the current formulation. This is particularly necessary as we have not yet fully justified some of the proposed "artificial symmetrisation". As well as applying such numerical tests, future work will also involve the introduction of approximate techniques to lead to efficient formulations for shells with large strains.

REFERENCES

Argyris, J. H., Balmer, H., Doltsnis, J. St., Dunne, P. C., Haase, M., Kleiber, M., Malejannakis, G. A., Mlejenek, J. P., Muller, M. and Scharpf, D. W. (1979). Finite element method—the natural approach. *Comp. Meth. in Appl. Mech. & Engng* **17/18,** 1–106.

Argyris, J. H. (1982). An excursion into large rotations. *Comp. Meth. in Appl. Mech. & Engng* **32,** 85–155.

Backlund, J. (1973). Finite element analysis of nonlinear structures. Ph.D. thesis, Chalmers Univ., Gotenburg, Sweden.

Belytschko, T. and Hseih, B. J. (1973). Non-linear transient finite element analysis with convected co-ordinates. *Int. J. Num. Meth. in Engng* **7,** 255–271.

Belytschko, T. and Glaum, L. W. (1979). Application of higher order corotational stretch theories to nonlinear finite element analysis. *Computers & Struct.* **10,** 175–182.

Bergan, P. G. and Felippa, C. A. (1986). Efficient implementation of a triangular membrane element with drilling freedoms. In *Finite Element Methods for Plate and Shell Structures* (Eds T.J.R. Hughes & E. Hinton), Vol. 1, Pinerdige Press, Swansea, pp. 128–152.

Celigoj, C. C. (private communication). A strain and displacement based variational method applied to geometrically nonlinear shells, Part 1 : Theoretical formulation.

Chen, K. K. (1979). A triangular plate finite element for large-displacement elastic-plastic analysis of automobile structural components. *Computers & Struct.* **10,** 203–215.

Crisfield, M. A. (1990). A consistent co-rotational formulation for non-linear three-dimensional beam elements. *Comp. Meth. in Appl. Mech. & Engng* **81,** 131–150.

Crisfield, M. A. (1991). *Non-linear Finite Element Analysis of Solids & Structures*, Vol. 1 ; Essentials. John Wiley, Chichester.

Crisfield, M. A. and Peng, X. (1992). Efficient nonlinear shell formulations with large rotations and plasticity. In *Computational Plasticity, Fundamentals & Applications*, Part 2 (Eds D.R.J. Owen *et al.*). Pineridge Press, Swansea, pp. 1979–1996.

Crisfield, M. A., Moita, G. F., Jelenic, G. and Lyons, L. P. R. (1995). Enhanced lower-order element formulations for large strains. In *Computational Plasticity, Fundamentals & Applications*, Part 1 (Eds D.R.J. Owen *et al.*). Pineridge Press, Swansea, pp. 293–320.

Crisfield, M. A. (to be published). *Non-linear Finite Element Analysis of Solids & Structures*, Vol. 2 ; *Advanced Topics*. John Wiley, Chichester.

Crisfield, M. A. and Moita, G. F. (submitted). A co-rotational formulation for 2-D including incompatible modes. *Int. J. Num. Methods in Engng.*

Herrmann, L. R. (1967). Finite element bending analysis of plates. *J. Engng Mech. Div., ASCE EM5* **93,** 13–25.

Horrigmoe, G. and Bergan, P. G. (1968). Nonlinear analysis of free-form shells by flat finite elements. *Comp. Meth. in Appl. Mech. & Engng* **16,** 11–35.

Hsiao, K.-M. (1987). Nonlinear analysis of general shell structures by flat triangular shell element. *Computers & Struct.* **25,** 665–675.

Irons, B. M. (1976). The semi-loof element. In *Finite Elements for Thin Shells and Curved Members* (Eds D.G. Ashwell *et al.*). Wiley, New York, pp. 197–222.

Jetteur, P. H. and Cescotto, S. (1991). A mixed finite element for the analysis of large inelastic strains. *Int. J. Num. Meth. in Engng* **31,** 229–239.

MacNeal, R. H. and Harter, R. L. (1988). A refined four-noded membrane element with rotational degrees of freedom. *Computers & Struct.* **28,** 75–88.

Moita, G. F. (1994). Nonlinear finite element analysis of continua with emphasis on hyperelasticity. Ph. D. Thesis, Imperial College, London.

Moita, G. F. and Crisfield, M. A. (submitted). A finite element formulation for 3-D continua using the co-rotational technique. *Int. J. Num. Meth. in Engng.*

Morley, L. S. D. (1971). The constant-moment plate-bending element. *J. Strain Analysis* **6,** 20–24.

Nour-Omid, B. and Rankin, C. C. (1991). Finite rotation analysis and consistent linearisation using projectors. *Comp. Meth. in Appl. Mech. & Engng* **93,** 353–384.

Nygard, M. K. and Bergan, P. G. (1989). Advances in treating large rotations for nonlinear problems. In *State of the Art Surveys on Computational Mechanics* (Eds A.K. Noor and T.J. Oden). ASME, New York.

Oran, C. (1973a). Tangent stiffness in plane frames. *J. Struct. Div., ASCE, ST6* **99,** 973–985.
Oran, C. (1973b). Tangent stiffness in space frames. *J. Struct. Div., ASCE, ST6* **99,** 987–1001.
Peng, X. and Crisfield, M. A. (1992). A consistent co-rotational formulation for shells using the constant stress/constant moment triangle. *Int. J. Num. Meth. in Engng* **35,** 1829–1847.
Rankin, C. C. and Brogan, F. A. (1986). An element independent corotational procedure for the treatment of large rotations. *ASME J. Pressure Vessel Technology* **108,** 165–174.
Simo, J. C., Fox, D. D. and Rafai, M. S. (1989a). On a stress resultant geometrically exact model, Part 1: Formulation and parametrisation. *Comp. Meth. in Appl. Mech. & Engng* **72,** 267–304.
Simo, J. C., Fox, D. D. and Rafai, M. S. (1989b). On a stress resultant geometrically exact model, Part 2: The linear theory; computational aspects. *Comp. Meth. in Appl. Mech. & Engng* **73,** 53–92.
Simo, J. C. and Rifai, M. S. (1990a). A class of assumed strain methods and the method of incompatible modes. *Int. J. Num. Meth. in Engng* **29,** 1595–1638.
Simo, J. C., Fox, D. D. and Rafai, M. S. (1990b). On a stress resultant geometrically exact model, Part 3: Computational aspects of the non-linear theory. *Comp. Meth. in Appl. Mech. & Engng* **79,** 21–70.
Simo, J. C., Armero, F. and Taylor, R. L. (1993a). Improved versions of assumed enhanced strain tri-linear elements for 3D finite deformation problems. *Comp. Meth. in Appl. Mech. & Engng* **110,** 359–386.
Simo, J. C. (1993b). On a stress resultant geometrically exact model, Part 7: Shell intersections with 5/6-DOF finite element formulation. *Comp. Meth. in Appl. Mech. & Engng* **108,** 319–339.
Taylor, R. L., Beresford, P. J. and Wilson, E. L. (1976). A non-conforming element for stress analysis. *Int. J. Num. Meth. in Engng* **10,** 1211–1219.
Van Keulen, F., Bout, A. and Ernst, L. J. (1993). Nonlinear thin shell analysis using a curved triangular element. *Comp. Meth. in Appl. Mech. & Engng* **103,** 315–343.
Wempner, G. (1969). Finite elements, finite rotations and small strains of flexible shells. *Int. J. Solids Struct.* **5,** 117–153.
Zienkiewicz, O. C., Parekh, C. J. and King, I. P. (1968). Arch dams analysed by a linear finite element shell solution program. In *Proc. Symp. on Arch Dams, Institution of Civil Engineers*, London.